Imaging 4 and 5 Dimensional Kerr-AdS Black Holes

David Carcamo

January 2020

Abstract

Understanding how light interacts with unique AdS Black Hole spactimes is imperative in understanding novel physics through the AdS/CFT correspondence. One way of understanding the motion of light around a black hole is to capture an image of the black hole. Therefore, we developed a method of imaging black holes in various spacetime geometries in both 4 and 5 dimensions. In this paper we present images of AdS_4 and AdS_5 kerr black holes.

1 Introduction

The anti-de Sitter/conformal field theory (AdS/CFT) correspondence has opened new ways of probing questions within quantum gravity. First discovered by Juan Maldacena in 1997, the AdS/CFT correspondence relates the boundary of an AdS spacetime to a Conformal Field Theory. The correspondence is best utilized when a problem on CFT side of the correspondence has an simpler representation on the AdS side and vice versa [1].

Anti-deSitter (AdS) Space is a spacetime with a negative cosmological constant. The effect of the cosmological constant cause photon path's to deviate from their trajectories in flat spacetime. Therefore, understanding what the images of a black hole within this AdS spacetime would look like can help elucidate new physics through the AdS/CFT correspondence. There have been previous attempts at simulating images of black holes in the past. Most notably would be the work that was done to simulate a black hole similar to the one that was imaged by the Event Horizon Telescope (EHT), which was the inspiration for this paper. There have been previous attempts at imaging higher dimensional black holes, however they focused on black holes in flat spacetimes [2].

In this paper, we generate the images of various 4 and 5 dimensional AdS spacetimes so that they might be used to understand the CFTs they generate.

2 Method

Traditional photography requires that light is either emitted or reflected from an object and travels to a camera sensor in order to be detected. However, a black hole adsorbs all light that it comes into contact with it. Further, the black hole directly affects the paths of photons that pass near by the black hole. In order to image the black holes in this paper, photons were sent perpendicular from the plane of the camera "sensor" towards the black hole. Following a similar method of color coding in [2], the photon paths were integrated until one of two events occurred: either the photon crossed the black hole's event horizon or it returns to the same radial distance as it was emitted. If the photon return to the same radial distance as it was admitted we color coded the position the photon returned to based off which quadrant its path ended in. Figure 1 illustrates the image the camera would take in empty space.

For reference, the inspiration for the numerical method used to create these images came from the video included in the New York Times article describing the work behind the Event Horizon Telescope [3].

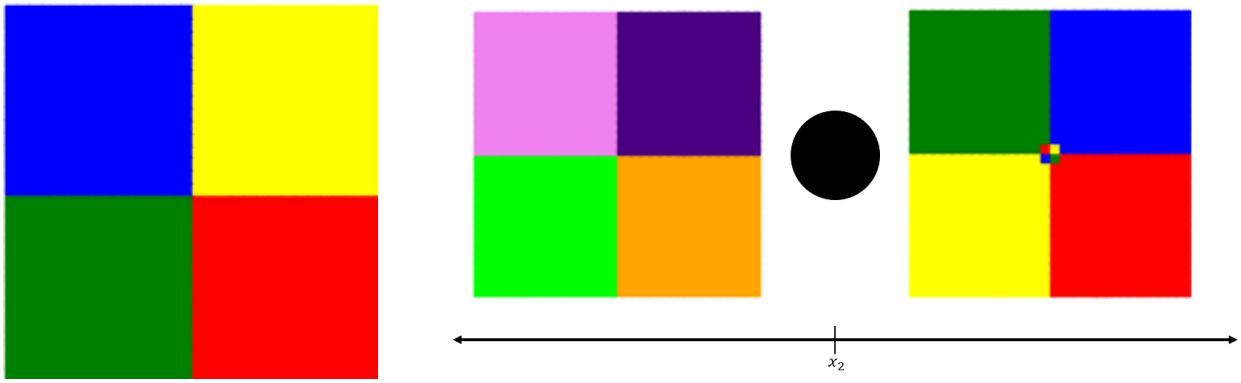

(a) 4D Empty

(b) 5D Empty

Figure 1: On the left is an image of empty 4D space. This image was generated by setting the mass and rotational parameters in the ads Kerr metric to zero. On the right is a representation of the image of empty 5D space. In order to convert our 3 spatial dimensional image to planar image we fixed one coordinate for the camera sensor to image. This is effectively a slice of the camera's 3 dimensional image. For reference, the black circle would represent the image of a black hole with the coloring of the 8 octants representing the cube surrounding the black hole. The defect in the center of the right half of the space is a error caused by the numerical integration. Each color represents the quadrant/octant that light would need to travel from in order to interact with our sensor.

2.1 Integration

In order to integrate the geodesics we followed the procedure in [4] where any time independent metric can be written in the form

$$g_{\mu\nu} = \begin{pmatrix} -\alpha^2 + \beta_k \beta^k & \beta_i \\ \beta_j & \gamma_{ij} \end{pmatrix} \tag{1}$$

where β_i is a three vector and γ_{ij} is the spatial component of $g_{\mu\nu}$. Writing the metric in this form allows for the geodesic equations to be written as a system of first order differential equations independent of the a particles proper time. The geodesic equations are written as a function of the spatial coordinates x^i and the contra-variant four velocity $u_i = g_{i\mu} u^\mu$ such that,

$$\frac{dx^i}{dt} = \gamma^{ij} \frac{u_j}{u_0} - \beta^i \tag{2}$$

$$\frac{du_i}{dt} = -\alpha u^0 \partial_i \alpha + u_k \partial_i \beta^k - \frac{u_j u_k}{2u_0} \partial_i \gamma^{jk} \tag{3}$$

where

$$u^0 = (\gamma^{jk} u_j u_k + \epsilon)^{1/2} / \alpha \tag{4}$$

with $\beta^i = \gamma^{ij} \beta_j$ and γ^{ij} is the inverse of γ_{ij}. For photon geodesics, $\epsilon = 0$. The convenience of using this method for solving the geodesics equations is the method used to integrate these metrics remains the same for any time independent metric. Additionally, in AdS space photons can travel the whole space in finite coordinate time. Meaning a photon can go from $x = -\infty$ to $x = +\infty$ in non-infinite time. Therefore, allowing us to set clear boundary conditions and stop the integration when the photon travels much longer than it takes to transverse the space. Further, while this method was originally designed for $3 + 1$ split metrics it generalizes further to $4 + 1$ metrics.

3 Camera Set Up

3.1 4D

The metrics used in this paper are best written in Boyer-Lindquist coordinates.

$$\begin{aligned} x_1 &= \sqrt{r^2 + a^2}\cos\phi\sin\theta, \\ x_2 &= \sqrt{r^2 + a^2}\sin\phi\sin\theta, \\ x_3 &= r\cos\theta \end{aligned} \tag{5}$$

The camera "sensor" has local coordinates (x, y, z), where the origin is the center of the camera's sensor. Similar to [2], we choose the coordinates of the camera as

$$(x^1, x^2, x^3)_{camera} = (d\sin i, 0, d\cos i) \tag{6}$$

where i is the angle of inclination between the x_1 and x_3 coordinate axes. This is illustrated in Figure 2a. Using this relation, we are able to map the null geodesic's initial position in the camera's coordinates to the initial position in the global coordinates.

To determine the initial velocity for the photon paths we used the convention of $c = 1$. The photons leave the camera sensor in the x direction of the the camera's local coordinates. Therefore, the spatial components of the photon's four velocity in the global coordinates are then $(-\sin i, 0 - \cos i)$. We then determined the components of the initial velocity of the photon so they leave the camera perpendicular to then sensor. We found the components of the initial velocity in (r_0, θ_0, ϕ_0) coordinates to be,

$$\begin{aligned} \dot{r}_0 &= -2\frac{(a^2 + r_0^2)\cos\theta_0\sin i + r_0\sqrt{a^2 + r_0^2}\cos i\cos\phi_0\sin\theta_0}{a^2 + 2r_0^2 + a^2\cos 2\theta_0}, \\ \dot{\theta}_0 &= 2\frac{r_0\sin\theta_0\sin i - \sqrt{a^2 + r_0^2}\cos i\cos\phi_0\cos\theta_0}{a^2 + 2r_0^2 + a^2\cos 2\theta_0}, \\ \dot{\phi}_0 &= \frac{\cos i\sin\phi_0}{\sin\theta_0\sqrt{a^2 + r_0^2}} \end{aligned} \tag{7}$$

3.2 5D

The same process to define the camera's initial setup in 4D was used for the 5D case. The major difference is the images generated were taken by fixing one of the camera's local coordinates. Therefore, the image displayed is a slice of the 3 dimension shadow of the 5D black hole. The global coordinates used to represent the metrics are again best written in Boyer-Lindquist coordinates.

$$\begin{aligned} x_1 &= \sqrt{r^2 + a^2}\cos\psi\sin\theta, \\ x_2 &= \sqrt{r^2 + a^2}\sin\psi\sin\theta, \\ x_3 &= \sqrt{r^2 + b^2}\cos\phi\cos\theta, \\ x_4 &= \sqrt{r^2 + b^2}\sin\phi\cos\theta, \end{aligned} \tag{8}$$

Following the same process as above, the canera sensor's local coordinates, (x, y, z, w), are related to the global coordinates in the following way

$$(x^1, x^2, x^3, x^4)_{camera} = (d\sin i, 0, d\cos i, 0) \tag{9}$$

where i is the angle of inclination between the x_1 and x_3 coordinates, best illustrated in Figure 2b. Similar to the 4D case, we launched the photons in the x direction in our camera's local frame. Following the same

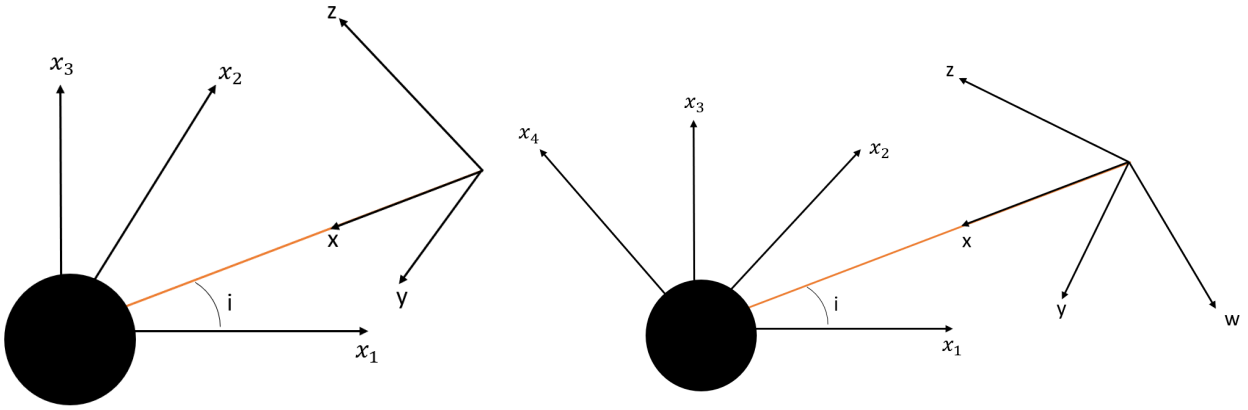

(a) 4 Space Time Dimensions

(b) 5 Space Time Dimensions

Figure 2: Schematic of the spatial relation of the camera sensor and the black hole to be imaged. On the left a 4D black hole sits at the origin of the global coordinates (x_1, x_2, x_3). Null rays emerges from the z-y plane with initial velocity in the x direction in the camera's coordinates. On the Right a 5D black hole sits at the origin of the global coordinates (x_1, x_2, x_3, x_4). Null rays emerges from the z-y-w cube with initial velocity in the x direction in the camera's coordinates. For imaging purposes, one of the dimensions of the camera's cubic sensor are compressed to make a 2 dimension image.

procedure as above, the initial velocities of the photons in terms of their initial position in the (r, θ, ψ, ϕ) global coordinates are:

$$\begin{aligned}
\dot{r}_0 &= \frac{\sqrt{r_0^2 + a^2}\left(\cos\theta_0 \cos\phi_0 \sin i + \cos i \cos\psi_0 \sin\theta_0\right)}{r_0} \\
\dot{\theta}_0 &= \frac{\cos\phi_0 \sin i \sin\theta_0 - \cos i \cos\psi_0 \cos\theta_0}{\sqrt{r_0^2 + a^2}} \\
\dot{\psi}_0 &= \frac{\cos i \sin\psi_0}{\sin\theta_0 \sqrt{a^2 + r^2}} \\
\dot{\phi}_0 &= \frac{\sin i \sin\phi_0}{\cos\theta_0 \sqrt{r_0^2 + a^2}}
\end{aligned} \tag{10}$$

4 Metrics

The Kerr-AdS$_4$ solution in Boyer-Linquist coordinates has the metric [5]:

$$\begin{aligned}
ds^2 &= -\frac{\Delta_r}{\xi^2}\left(dt - \frac{a}{\Xi}\sin^2\theta d\phi\right)^2 + \frac{\xi^2}{\Delta_r}dr^2 + \frac{\xi^2}{\Delta_\theta}d\theta^2 + \frac{\Delta_\theta \sin^2\theta}{\xi^2}\left(adt - \frac{r^2 + a^2}{\Xi}d\phi\right)^2, \\
\Delta_r(r) &= \left(r^2 + a^2\right)\left(1 + \frac{r^2}{l_{ads}^2}\right) - \frac{1}{r_+}(r_+^2 + a^2)\left(1 + \frac{r_+^2}{l_{ads}^2}\right) r, \\
\Delta_\theta(\theta) &= 1 - \frac{a^2}{l_{ads}^2}\cos\theta, \\
\xi^2(r, \theta) &= r^2 + a^2\cos^2\theta, \\
\Xi &= 1 - \frac{a^2}{l_{ads}^2}.
\end{aligned} \tag{11}$$

We used the same coordinate system as defined in Equation 5 where a is the rotational parameter with the black hole rotating in the $x_1 - x_2$ plane, l_{ads} is the AdS length scale, and r_+ is the radius of black hole

event horizon. The mass parameter of this black hole is therefore $\mu = \frac{1}{r_+}(r_+^2 + a^2)(1 + \frac{r_+^2}{l_{ads}^2})$. In order to find the extremal limit of this black hole we need to find the limit where the temperature of the black hole approaches zero. From [6], the black hole temperature is:

$$T_{AdS-Kerr_4} = \frac{r_+ \left(1 + a^2 l^{-2} + 3r_+^2 l^{-2} - a^2 r_+^2\right)}{4\pi(r_+^2 + a^2)} \tag{12}$$

By requiring both the temperature to be positive, $T \geq 0$, and the rotation of the black hole to be $a \leq 1$[1] we find a to be

$$a \leq \begin{cases} \sqrt{\frac{l^2+3r_+^2}{l^2-r_+^2}}, & r_+ \leq \frac{l}{\sqrt{3}} \\ 1, & r_+ > \frac{l}{\sqrt{3}} \end{cases} \tag{13}$$

By now requiring $T = 0$ we find the extremal limit to be when $r_+ \leq \frac{l}{\sqrt{3}}$ and $a = \sqrt{\frac{l^2+3r_+^2}{l^2-r_+^2}}$.

The Kerr-AdS$_5$ solution in Boyer-Linquist coordinates has the metric [5]:

$$\begin{aligned}
ds^2 = &-\frac{\Delta_r}{\xi^2}\left(dt - \frac{a}{\Xi_a}\sin^2\theta d\psi - \frac{b}{\Xi_b}\cos^2\theta d\phi\right)^2 + \frac{\xi^2}{\Delta_r}dr^2 + \frac{\xi^2}{\Delta_\theta}d\theta^2 \\
&+ \frac{\Delta_\theta \sin^2\theta}{\xi^2}\left(adt - \frac{r^2+a^2}{\Xi_a}d\psi\right)^2 \\
&+ \frac{\Delta_\theta \cos^2\theta}{\xi^2}\left(bdt - \frac{r^2+b^2}{\Xi_b}d\phi\right)^2, \\
&+ \frac{1 + r^2 l^-2_{ads}}{r^2\xi^2}\left(abdt - \frac{b(r^2+a^2)\sin^2\theta}{\Xi_a}d\psi - \frac{a(r^2+b^2)\cos^2\theta}{\Xi_b}d\psi\right)^2, \\
\Delta_r(r) = &\frac{1}{r^2}(r^2+a^2)(r^2+b^2)(1+\frac{r^2}{l_{ads}^2}) - \frac{1}{r_+^2}(r_+^2+a^2)(r^2+b^2)(1+\frac{r_+^2}{l_{ads}^2}), \\
\Delta_\theta(\theta) = &1 - \frac{a^2}{l_{ads}^2}\cos\theta, \\
\xi^2(r,\theta) = &r^2 + a^2\cos^2\theta, \\
\Xi_a = &1 - \frac{a^2}{l_{ads}^2}, \\
\Xi_b = &1 - \frac{a^2}{l_{ads}^2}.
\end{aligned} \tag{14}$$

Using the coordinate system defined in 8, the black hole has two independent rotational parameters. Therefore, the rotational parameter a denotes the rotation in the $x_1 - x_2$ plane and b represents the rotation in the $x_3 - x_4$ plane.

Again to understand the extremal limits of this spacetime we need to find when $T_{AdS_5} = 0$. The temperature of an AdS$_5$ black hole is defined as

$$T_{AdS_4} = \frac{1}{2\pi}\left[r_+\left(1 + \frac{r_+^2}{l^2}\right)\left(\frac{1}{r_+^2+a^2} + \frac{1}{r_+^2+b^2}\right) - \frac{1}{r_+}\right] \tag{15}$$

In the case where the black hole is spinning around a single axis, the temperature is strictly positive. Therefore, the black hole can become extremal only if and only if it is rotating around both axis of rotation. For the case when the black hole has equal rotation in both planes of rotation we find the extremal limit as

[1]This condition is chosen so that the boundary rotates slower than the speed of light

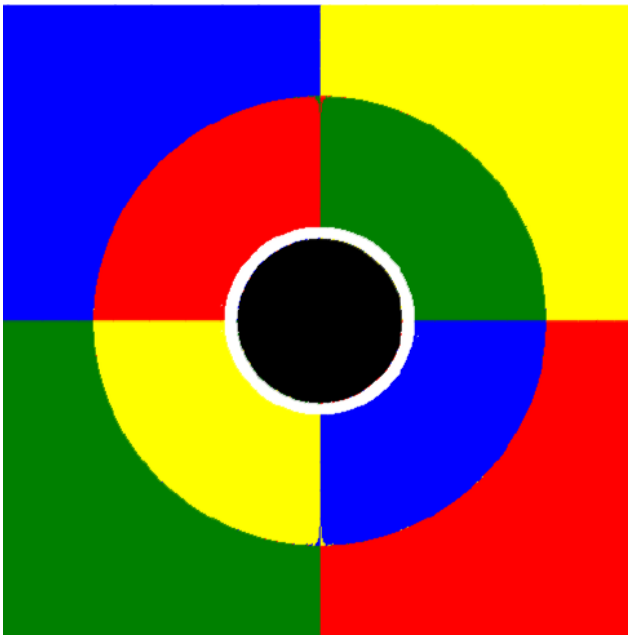

Figure 3: High Resolution Image of a standard Schwarzschild Black Hole

$$a = b = r_+\sqrt{1+2r_+^2}, r_+ \leq \frac{1}{\sqrt{2}} \tag{16}$$

Of course it is not necessary for the two rotational parameters to be equal for the black hole to be extremal. However, there is no analytical expression for the black hole radius in the non-equally rotating case.

5 Images

5.1 4D

As a proof of concept, we created a high-resolution, 512x512 pixels, image of a Schwarzschild Black Hole. The eventual goal of this project will be to generate all images at these resolutions, see Figure 3. However, the time to generate a high resolution image is on the order of a day. Even after considerable improvements to the computational method, including generating pixel in parallel on a quad core CPU, each image will take about 8 hours to simulate. Therefore, all further images are of lower resolution, 100x100 pixels, for comparison purposes. In this image, we can see in detail how photons are bent around the black hole. The white pixels represent photons that are bent around the black hole and come back to the camera. Therefore, we can see the thin photon ring that would surround any Schwarzschild Black Hole.

The main purpose of this project is to understand the geometries generated by complex Black Hole AdS spacetimes. An example of such an extreme spacetime is nearly maximally spinning Kerr-AdS$_4$. As seen in figure 4b, the image of the black hole shows the how extreme the effect of the AdS lensing coupled with the rotation of the black hole is on the path of the photons. Compared to figure 4a, which depicts a relatively slow spinning black hole, the faster the black hole spins the larger the event horizon appears. However, the event horizon imaged is not the true event horizon. These images tell us that the light coming from one end of the spacetime will have less of an effect on the boundary on the opposite end. Even further, these images show that in a maximally spinning AdS-Kerr spacetime there would be no causal relationship between the boundary of the spacetime and any other point on the boundary. Lastly, we see the spin of the Black Hole breaks the planar symmetry of the space.

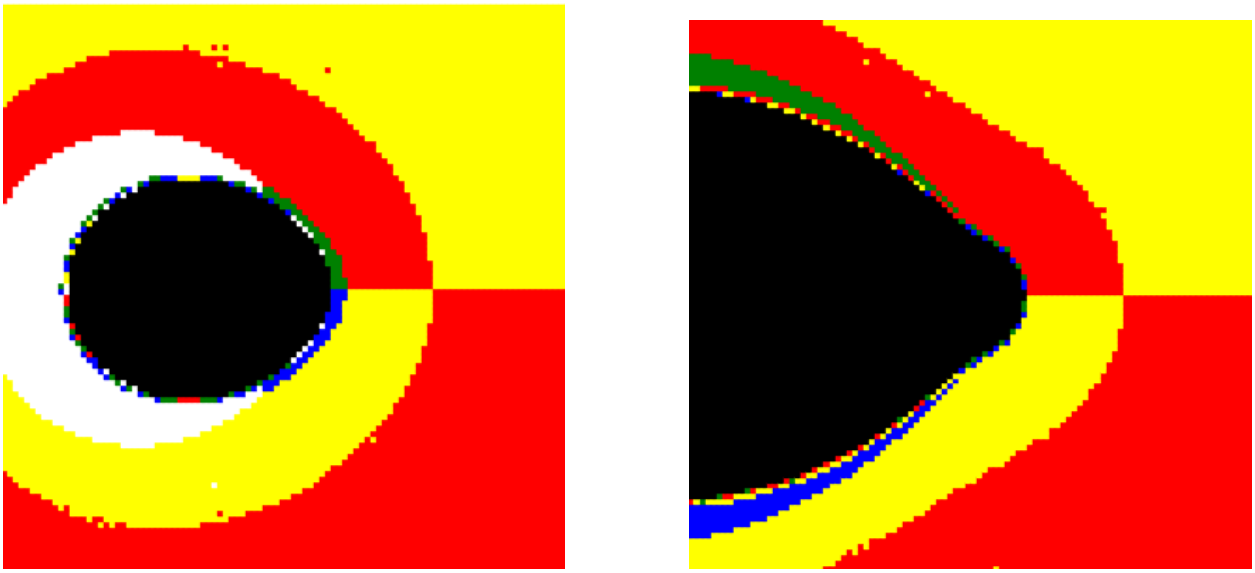

(a) Slow Spinning Kerr- AdS_4

(b) Fast Spinning Kerr- AdS_4

Figure 4: On the right is a 4D Kerr-AdS black hole with spin of 0.6 and a radius of 0.5 in units of the AdS length scale. Maximal spin for this black hole is near 0.763. On the left is a larger black hole with radius 1 and spin 0.3. For both black holes the axis of rotation is parallel to the plane of the image.

5.2 5D

The major difference between imaging in 4 dimensions and 5 dimensions is the image of a 5 spacetime dimensional object would create a 3 spatial dimensional image. In order to show this image on paper, we decided to slice this 3 spatial dimensional object into 2 spatial dimension slices. By doing this, we can view the image in the same manor as viewing slices of an MRI image.

For the sake of brevity, we will only illustrate one example of AdS_5. Figure 5 shows the cross sections of a rotating Kerr-AdS_5 Black Hole. Interestingly, we see three distinct rings around the black hole. As expected there is still a faint photon ring that orbits the black hole. Additionally, we see two distinct rings. These rings show how lights coming from the dimension perpendicular to the ones shown are twisted into one another. Unlike the 4 dimensional case, the size of these regions are symmetric across the plane.

There is no maximum rate of rotation for a 5 dimension Kerr Black Hole. Therefore, we see Kerr Black Holes in flat space time appear to remain the same size as the rate of rotation increases. However, in AdS space there is a maximum speed for Kerr Black Holes. As in the 4 dimensional case, our work shows (not depicted) the event horizon and the photon ring increase in size as the black hole spins approach the maximum. This implies that there are no causal links between opposite sides of the spacetime as the black holes approach extrema.

6 Conclusion

In this paper we have demonstrated a method for imaging black holes in higher dimensions. Using this method we investigated the properties of Kerr-AdS Black Holes in 4 and 5 dimensions. We found that as the spin of the Black Holes approach extrema the warping of the spacetime prevents any causal connection between opposite ends of the spacetime. In the future, we plan on using these observations to investigate how the physics that is described by the CFT on the boundary of the spacetime is affected by the lack of causal links.

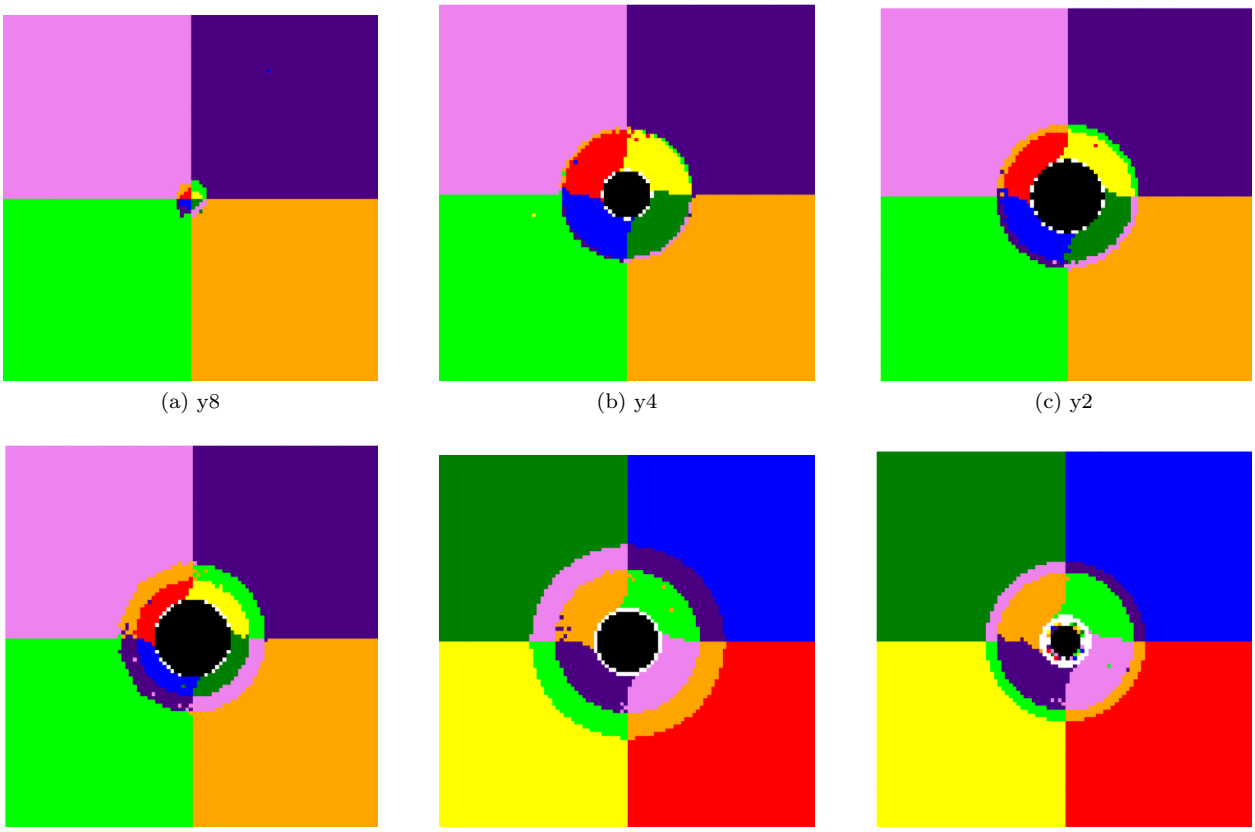

(a) y8 (b) y4 (c) y2

(d) y1 (e) y-1 (f) y-2

Figure 5: Here we demonstrate slicing through the 3 spatial dimension image of a rotating Kerr-AdS$_5$ Black Hole. The Center of the image is located at y0, in units of AdS length. This particular black hole is rotating around two axes with rotational speed of 1 around both and has a radius of 1.

7 Acknowledgements

I would like to thank the University of California Davis REU program for giving me the opportunity to participated in this research. In particular I would like to thank Dr. Zieve, Dr. Mahoney, and Dr. Scalettar for organizing this program and creating a sense of community during this epidemic.

Lastly, I would like to thank my advisor Dr. Rangamani for his guidance and input on this project.

References

[1] Jared Kaplan. *Lectures on AdS/CFT from the Bottom Up.* 2016. URL: https://sites.krieger.jhu.edu/jared-kaplan/files/2016/05/AdSCFTCourseNotesCurrentPublic.pdf.

[2] Thomas Hertog, Tom Lemmens, and Bert Vercnocke. "Imaging higher-dimensional black objects". In: *Physical Review D* 100.4 (2019). DOI: 10.1103/physrevd.100.046011.

[3] Dennis Overbye. "Infinite Visions Were Hiding in the First Black Hole Image's Rings". In: *New York Times* (Mar. 2020). URL: www.nytimes.com/2020/03/28/science/black-hole-rings.html.

[4] F. Bacchini et al. "Generalized, Energy-conserving Numerical Simulations of Particles in General Relativity. I. Time-like and Null Geodesics". In: *The Astrophysical Journal Supplement Series* 237.1 (2018), p. 6. DOI: 10.3847/1538-4365/aac9ca.

[5] G.w. Gibbons et al. "The general Kerr-de Sitter metrics in all dimensions". In: *Journal of Geometry and Physics* 53.1 (2005), pp. 49–73. DOI: 10.1016/j.geomphys.2004.05.001.

[6] G W Gibbons, M J Perry, and C N Pope. "The first law of thermodynamics for Kerr–anti-de Sitter black holes". In: *Classical and Quantum Gravity* 22.9 (2005), pp. 1503–1526. DOI: 10.1088/0264-9381/22/9/002.